FEM SIMULATION OF AN INTEGRATED LONGITUDINAL AND TANGENTIAL WAVE PROBE

P. Hora [*], **O. Červená** [**]

Abstract: *The aim of contribution is the finite element modeling of integrated longitudinal and shear wave probe. This type of probe was investigated by Cheng-Kuei Jen and Makiko Kobayashi in Jen (2007). Finite element calculations are performed in the commercial environment COMSOL Multiphysics. The ultrasonic transducer excitation was modeled as total force load. The received ultrasonic signal was obtained by integration of velocities at place of ultrasonic transducer. Though these simplifications the resulting ultrasonic signals are in good agreement with results presented by Cheng-Kuei Jen and Makiko Kobayashi.*

Keywords: ***Ultrasonic probe, FEM modeling.***

1. Introduction

Non-destructive testing (NDT) of materials are commonly performed to identify and characterize of defects and damage in metals, metal alloys, composites and other materials. Furthermore, the increasing demand to improve the performance, increase reliability and extend the life of transportation vehicles, structures and engineering systems, requires the use of systems that have integrated capabilities with built-in sensors that perceive and process in-service information and take actions to accomplish desired operations and tasks. It is established that ultrasonic methods are widely used for real-time, in-situ or off-line NDT and evaluation of large metallic and composite structures including airplanes, pressure vessels and pipelines, Kundu (2004).

Because of their subsurface inspection capability, elastic property characterization ability, fast inspection speed, simplicity and cost-effectiveness, there has been considerable interest in ultrasonic NDT. Common limitations of current piezoelectric ultrasonic transducers (UT) are (a) lack of suitability for use on curved surfaces and (b) the difficulty for use at temperatures higher than 100°C. Therefore the objective of this investigation is to develop integrated longitudinal, shear, Rayleigh surface and Lamb plate acoustic wave transducers and flexible high temperature UT operated at least up to 150°C, Jen (2007).

2. Integrated longitudinal and shear wave probe

Various efforts have been devoted to the development of piezoelectric UTs of large bandwidth and high efficiency and they may be supplied by several companies. However, it is understood that S waves may be advantageous over P waves for NDT and characterization of materials because liquid and gas medium do not support S waves. In addition, for the evaluation of material properties, sometimes it is important to measure shear modulus and viscoelastic properties in which S wave properties are a requisite. Furthermore, a UT setup to generate and receive both P and S waves at the same sensor location would be also of interest.

The mode conversion from P to S wave due to reflection at a solid-air interface was reported in Achenbach (1973); Graff (1975). It means that the P wave UT together with P-S mode conversion caused by the reflection at a solid-air interface can be effectively used as a S wave probe as shown in Fig. 1. P waves in this figure generated by an P wave UT reach a solid-air interface and reflected as PP

[*]Doc. Ing. Petr Hora, CSc.: Institute of Thermomechanics AS CR, v. v. i., Dolejškova 1402/5; 182 00, Prague; CZ, e-mail: hora@cdm.it.cas.cz

[**]RNDr. Olga Červená: Institute of Thermomechanics AS CR, v. v. i., Dolejškova 1402/5; 182 00, Prague; CZ, e-mail: cervena@cdm.it.cas.cz

and PS waves. The equations governing the reflection and mode conversion with respect to the P wave incident angle α can be given in Eqs.1-3, Achenbach (1973); Graff (1975), where c_1 and c_2 are P and S wave velocities in the solid, respectively, and R_{PP} and R_{PS} are energy reflection coefficients of the P and S waves, respectively.

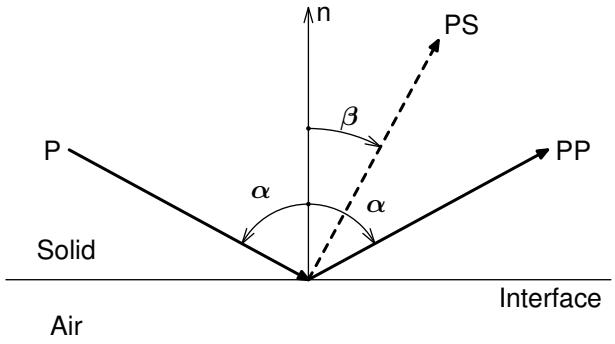

Fig. 1: Reflection and mode conversion wave at solid–air interface.

$$\frac{c_1}{\sin\alpha} = \frac{c_2}{\sin\beta} \tag{1}$$

$$R_{PP} = \left(\frac{\cos^2 2\beta - (c_2/c_1)^2 \sin 2\alpha \sin 2\beta}{\cos^2 2\beta + (c_2/c_1)^2 \sin 2\beta \sin 2\alpha} \right)^2 \tag{2}$$

$$R_{PS} = \frac{4\,(c_2/c_1)^2 \cos^2 2\beta \sin 2\alpha \sin 2\beta}{\left(\cos^2 2\beta + (c_2/c_1)^2 \sin 2\beta \sin 2\alpha \right)^2} \tag{3}$$

In this study, a steel with the P wave velocity c_1 = 5770.8 m/s and S wave velocity c_2 = 3138.5 m/s at room temperature was used as the substrate. These values are corresponding to the elastic properties of the substrate material in FEM analysis. Fig. 2 depicts the relation of angle of reflection to angle of incidence. The used angles of incidence are plotted by dashed lines. Fig. 3 shows the calculated energy reflection coefficient based on Eqs. 2 and 3 for the mild steel substrate. It indicates that the maximum energy conversion rate from the P wave to the PS wave is 97.8% at α = 67.3°, and the reduction of the energy conversion rate is within 1% in the α range between 60.8° and 73.0°.

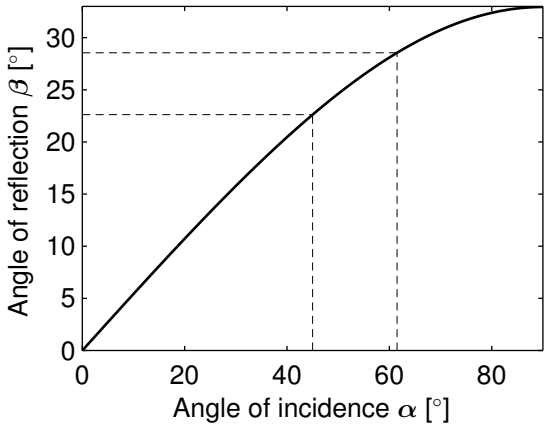

Fig. 2: Angle of reflection (β) vs. angle of incidence (α).

By considering this criterion, $\alpha + \beta$ is required to be 90°. From Eq. 1, which is the Snell's law, we can obtain α = 61.46° ($\alpha = \arctan(c_1/c_2)$). At this angle, the conversion rate is 97.03% that is

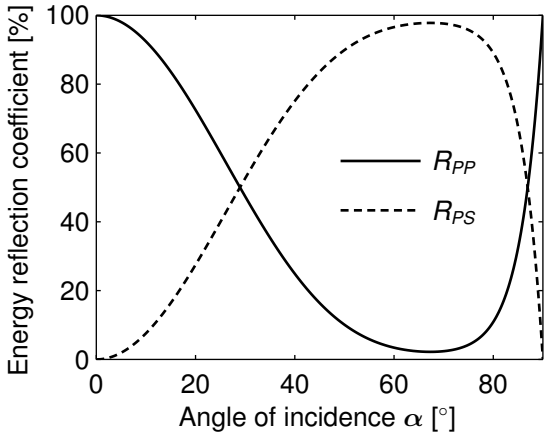

Fig. 3: Energy reflection coefficient vs. angle of incidence (α).

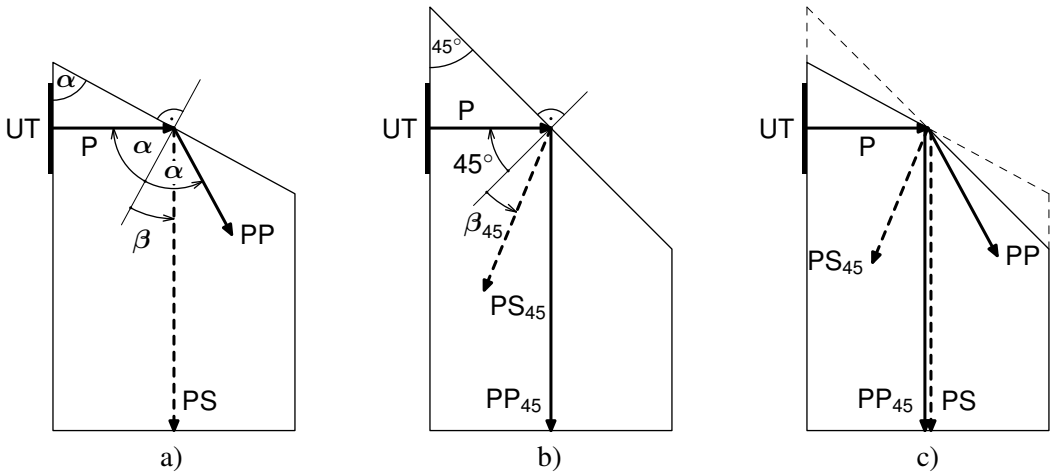

Fig. 4: Cases of the studied ultrasonic probes.

only 0.79% smaller than the maximum conversion rate at 67.3°, based on the result in Fig.3. Therefore, Fig. 4a) shows the schematic design developed for this study.

In Fig. 4b) the schematic diagram of an integrated P wave UT probe with the P wave UT is located in a plane parallel to the direction of PP wave where $\alpha = 45°$ is shown.

In Jen (2007) is shown, how to generate and receive both P and S waves at the same time. The S wave probe shown in Fig. 4a) can be modified to achieve such a purpose. In fact, it simply makes a slanted surface with an angle 45° from the intersection of the slanted plane and the line from the center of the P UT as shown in Fig. 4c). The 45° angle plane will reflect the energy of the P wave into the PP_{45} wave normal to the probing end as shown in Fig. 4c). Therefore, in principle, the upper part of the P wave, generated from P UT, can be used to produce the PS wave and the lower part to produce the PP_{45} wave.

3. FEM modeling

FEM modeling was performed for all three cases of probes depicted in Fig. 4. FE time dependent calculations are performed in the commercial environment COMSOL Multiphysics with the Structural Mechanics Module, COMSOL (2012). The plane strain was used as an application mode.

The probe width was 16 mm and middle of P UT (h) was located at 20 mm from probe end for each cases. The P UT size (w) was 6 mm. The steel with Young's modulus 200 GPa, Poisson's ratio 0.29 and density 7870 kg/m^3 was chosen as the substrate material of probe.

The quadrilateral mapped mesh with maximal element edge 0.2 mm is created. Elements are the Lagrange–Quadratic type. Number of elements for case a) and c) was 9760, for case b) was 11200. Number of degrees of freedom for case a) and c) was 78890, for case b) 90482.

The P UT was modeled as total force load in x-direction:

$$F_x(t,y) = \cos^2\left(\frac{y-h}{w}\pi\right)(1-\cos(2\pi ft/N))\sin(2\pi ft), \quad t \in \langle 0, 1\mu\text{s}\rangle, \quad y \in \langle h - w/2, h + w/2\rangle$$

where f = 5 MHz is frequency, N = 5 is number of cycles, and t is time. The others edges were free.

Calculations were done in time interval from 0 to 30 μs with time step 0.01 μs. Relative tolerance of solution was 1×10^{-4}, absolute tolerance 1×10^{-8}. Method BDF with maximum BDF order equals to 2 was used for this time analysis. The received ultrasonic signal was obtained by integration of velocities at place of ultrasonic transducer.

4. Conclusions

The contribution deals with the finite element modeling of integrated longitudinal and shear wave probe that was described by Cheng-Kuei Jen and Makiko Kobayashi. Finite element calculations were performed for three cases of probes: the first one used the reflected S wave, the second one the reflected P wave and the third one used both S wave and P wave. The ultrasonic transducer excitation was modeled as total force load. The integration of velocities at place of ultrasonic transducer was used as the received ultrasonic signal.

The effect of the reflected PP wave for cases a) and c) is negligible due to the low value of the energy reflection coefficient $R_{PP} \approx 3\%$ for given angle of incidence α = 61.46°. The influence of the reflected PS_{45} wave for cases b) and c) is insignificant because of the dimension of the substrate has been chosen so that the reflected PS_{45} wave from the probing end does not enter into the aperture of the P UT. Though some simplifications the results are in good agreement with work of Cheng-Kuei Jen and Makiko Kobayashi.

The analyze of the P UT size and location will be our further aim. The area of the P UT will be adjusted so that the amplitudes of the reflected PS and PP_{45} waves will be nearly the same.

Acknowledgments

The work has been supported by the Institute Research Plan AV0Z20760514 and by the grants GA CR No 101/09/1630.

References

Jen, Ch.-K., Kobayashi, M., (2007), Integrated and Flexible High Temperature Piezoelectric Ultrasonic Transducers. In: *Ultrasonic and advanced methods for nondestructive testing and material characterization* (C.H. Chen ed.) Wolrd Scientific, New York, chap. 2

Kundu, T., (2004), *Ultrasonic Nondestructive Evaluation: Engineering and Biological Material Characterization*, CRC Press, New York.

Achenbach, J. (1973), *Wave Propagation in Elastic Solids*, North-Holland, New York.

Graff, K.F. (1975), *Wave Motion in Elastic Solids*, Dover, New York.

COMSOL, Inc., http://www.comsol.com